Geosci. Model Dev. Discuss., doi:10.5194/gmd-2016-29, 2016
Manuscript under review for journal Geosci. Model Dev.
Published: 19 February 2016

Geoscientific Model Development Discussions
Open Access
EGU

A land surface model combined with a crop growth model for paddy rice (MATCRO-Rice Ver. 1) – Part II: Model validation

Yuji Masutomi[1], Keisuke Ono[2], Takahiro Takimoto[2], Masayoshi Mano[3], Atsushi Maruyama[4], and Akira Miyata[2]

[1]College of Agriculture, Ibaraki University, 3-21-1, Chuo, Ami, Inashiki, Ibaraki 300-0393, Japan
[2]National Institute for Agro-Environment Sciences, 3-1-3, Kannondai, Tsukuba, Ibaraki 305-8604, Japan
[3]Graduate School of Horticulture, Chiba University, 648 Matsudo, Matsudo-shi, Chiba 271-8510, Japan
[4]National Agriculture and Food Research Organization, 3-1-1 Kannondai, Tsukuba, Ibaraki 305-8666, Japan

Correspondence to: Yuji Masutomi (yuji.masutomi@gmail.com)

Abstract. We conducted a comprehensive validation of the simulations by MATCRO-Rice developed by Masutomi et al. (2016). In the validation, we compared simulations with observations for latent heat flux (LHF), sensible heat flux (SHF), net carbon flux, and paddy rice yield from 2003 to 2006. The observation site used for the comparison is located in Tsukuba, Japan, where inputs for running the model and outputs for the validation were fully observed. The 4-year average root mean square errors (RMSEs) between simulations and observations for LHF and SHF were 18.57 and 12.66 W m^{-2}, respectively. These values for errors are comparable to those reported in earlier studies. The comparison of biomass growth during growing periods from 2003 to 2006 shows that the simulations were in agreement with the observations, indicating that the model can reproduce the net carbon flux well. The 4-year average RMSE for crop yield in the same period was 402.4 kg ha^{-1}, which accounted for 7.9% of the mean observed yields. These results indicate that MATCRO-Rice has high ability to accurately and consistently simulate LHF, SHF, net carbon flux, and crop yield.

1 Introduction

It has been recognized that crop growth and management in agricultural land are important factors that affect climate at various spatial and temporal scales via exchange of heat, water, and gases (Tsvetsinskaya et al., 2001;Bondeau et al., 2007; Osborne et al., 2009; Levis et al., 2012). Betts (2005) pointed out that integration of crop growth models (CGMs) into climate models is needed for accurate climate simulations by climate models. To consider the influence of agricultural land on climate in climate simulations, several land surface models (LSMs) or dynamics vegetation models (DVMs) incorporated with a CGM have been developed (Tsvetsinskaya et al., 2001; Kucharik, 2003; Gervois et al., 2004; Bondeau et al., 2007; Osborne et al., 2007; Lokupitiya et al., 2009; Maruyama and Kuwagata, 2010; Levis et al., 2012; Osborne et al., 2015).

Masutomi et al. (2016) have developed a new LSM-CGM combined model, called MATCRO-Rice. The most important feature of the model is that it can consistently simulate latent heat flux (LHF), sensible heat flux (SHF), net carbon flux, and crop yield in paddy rice fields by exchanging variables between an LSM and a CGM. The consistency among model outputs enable us to apply the model to a wide range of integrated issues. For example, the model can investigate the interaction

Geosci. Model Dev. Discuss., doi:10.5194/gmd-2016-29, 2016
Manuscript under review for journal Geosci. Model Dev.
Published: 19 February 2016

between climate and paddy rice fields, consistently considering impacts of climate on rice productivity and impacts of paddy rice fields on climate. Osborne et al. (2009) showed that this interaction can affect variability in climate and crop production. Therefore, the understanding of the interaction is important for securing food security. However, little is known about the interaction. MATCRO-Rice can be a useful tool to study the interaction between climate and paddy rice fields.

The objective of the present paper is to present the results of the comprehensive validation of MATCRO-Rice. Using observations in a flux site, where the inputs to run the model and the outputs for the validations are fully observed, we compare the simulations with the observations for LHF, SHF, net carbon flux, and rice yield from 2003 to 2006. We first introduce the data and method used for the validation. Second, we explain the details of the parameterisation method in Section 3. Then, we show the results of the validation in Section 4 and finally present concluding remarks in Section 5

2 Data and method

2.1 Site and observational data

The observational flux site used for the model validation is located in Tsukuba, Japan (Lat: 36° 03' 14.3" N; Long: 140° 01' 36.9" E), at 13 m above sea level. The climatic zone is temperate, with the mean annual air temperature 13.7°C and precipitation 1200 mm. The soil type is clay loam. Table 1 shows the values of soil parameters for clay loam. The planting method used was transplanting.

All data required for running and validating the model for the period from 2003 to 2006 were observed at the site. Table 2 shows the observational data used for the validation. Information on the instruments used for the observations are available from the AsiaFlux web site (AsiaFlux, 2016). The height at which the wind speed was measured was different each year. Assuming logarithmic vertical profile of the wind, we transformed the observed wind speed to that at 3 m above ground and used the transformed wind speed for model inputs. Biomass for each organ (W_{lef}, W_{pnc}, W_{rot}, and W_{stm}) and leaf area index (L) were measured nearly every two weeks. At each measuring time, ten stands were sampled from the fields. Yield (Yld) and phenological dates including transplanting (Tr_{DOY}), heading (Hd_{DOY}), and harvest (Hv_{DOY}) were observed every year. The values of observed yield are the husked rice yield with 15% water content. The rice grains for measuring yield were sampled from the whole fields of the observational site. The crop height (h_{gt}) was measured on average every 5 days. It is noted that we used the observed values of photosynthesis active radiation (PAR) in addition to the standard meteorological inputs in the model validation.

2.2 Numerical setting and method

The values for all simulation setting parameters are shown in Table 3. We set the time resolution of the simulation to half hour, i.e., $\delta_t = 1800$. For time discretisation, the forward difference method was used.

To simulate soil water and heat transfer, we spatially discretised soil into five layers with thickness of 0.05, 0.2, 0.75, 1.0, and 2.0 m, resulting in $z_{max} = 4.0$ m, $z_{sat} = 0.05$ m, and $z_b = 2.0$ m. To simulate soil water content for each soil layer (w_s),

Geosci. Model Dev. Discuss., doi:10.5194/gmd-2016-29, 2016
Manuscript under review for journal Geosci. Model Dev.
Published: 19 February 2016

Geoscientific Model Development Discussions

we replaced the gradient of water flux by net water fluxes between layers. In the calculation for water fluxes between layers, we used the hydraulic conductivity averaged between soil layers and the difference in water potentials between soil layers. After the calculation for soil water content for each layer, water content beyond saturation was taken out to base flow.

To simulate soil temperature for each soil layer, we solved the system of equations for soil layers by using the Gauss-Jordan method. In the calculation of soil temperatures, we replaced the gradient of heat flux by net heat fluxes between layers. In the calculation of heat fluxes between layers, we used thermal conductivity averaged between soil layers and soil temperatures for each layer.

The downhill simplex method (Nelder and Mead, 1965) was used to simulate temperatures of the canopy and surface water (T_c and T_w), bulk transfer coefficients (C_{Ew}, C_{Ec}, C_{Hw}, C_{Hc}, C_M, and C_{Mw}), and variables related to carbon assimilation ($\overline{A}_{n,x}, c_{i,x}$, and $\overline{g}_{st,x}$) .

We set z_a = 3, because the wind speed for model inputs was measured at 3 m, as explained in Section 2.1. L_{at} was set to 36.05° according to site location (Section 2.1). CO_2 concentration (C_a) and the depth of surface water (d_w) were set at 390 ppm and 0.025 m, respectively. The initial dry weight of each organ was set at 1 kg ha^{-1} for leaf ($W_{lef,0}$), stem ($W_{stm,0}$), and root ($W_{rot,0}$) and at 0.5 kg ha^{-1} for glucose reserve in leaf. Sw_{DOY} was calculated from the observed transplanting date (Tr_{DOY}), assuming that transplanting was conducted 20 days after sowing, i.e., $Sw_{DOY} = Tr_{DOY} - 20$.

3 Parameterisation

3.1 Rubisco-limited photosynthesis rate

Parameters related to Rubisco-limited photosynthesis rate ($V_{max}(0)$, s_1, and s_2) were parameterised. In this parameterisation, we adjusted the parameters so that the Rubisco-limited photosynthesis rate ($\overline{\omega}_{c,x}$) simulated by MATCRO agrees with the observational value reported by Borjigidai et al. (2006). In the simulations, CO_2 concentration in the leaf was fixed to $c_{i,x} = 30$ Pa. Parameterised values are listed in Table 4. Figure 1, showing the comparison of Rubisco-limited photosynthesis rates among MATCRO, those reported by Borjigidai et al. (2006), and MATSIRO (Takata et al., 2003), on which MATCRO is based, indicate that there is a good agreement in the photosynthesis rate between the simulations of MATCRO and the observational value in Borjigidai et al. (2006); the simulations for the photosynthesis rate of MATCRO were significantly improved compared to those of MATSIRO. However, MATCRO had a tendency to overestimate the photosynthesis rate at lower temperature. This point should be improved by further parameterisation.

3.2 Phenology

Phenological parameters that represent development stages ($eDVS$, $hDVS$, $mGDS$, $trDVS$, and $teDVS$) were parameterised. First, we calculated DVSs at heading and $mGDS$s from 2003 to 2006 using the phenological model given by Masutomi et al. (2016). The mean values were set to $hDVS$ and $mGDS$, resulting in $hDVS = 0.616$ and $mGDS = 167759940$. Figure 2 compares the heading and harvest dates between observations and simulations from 2003 and those from 2006. The

Geosci. Model Dev. Discuss., doi:10.5194/gmd-2016-29, 2016
Manuscript under review for journal Geosci. Model Dev.
Published: 19 February 2016

Geoscientific Model Development Discussions

simulated heading and harvest dates were in good agreement with the observations. The average errors were 2.25 and 4.5 days for heading and harvest, respectively.

$eDVS$, $trDVS$, and $teDVS$ were determined so that the duration from sowing to emergence, transplanting, and the end of transplanting shock was 5, 20, and 25 days, respectively. Thus, $eDVS = 0.012$, $trDVS = 0.06$, and $teDVS = 0.08$.

3.3 Partitioning

Parameters related to glucose partitioning (DVS_{rot1}, DVS_{rot2}, DVS_{lef1}, DVS_{lef2}, DVS_{pnc1}, DVS_{pnc2}, P_{rot}, and P_{lef}) were parameterised as follows: (i) we calculated the ratio of glucose partitioned to each organ (leaf, stem, root, panicle) during the growing period using the observed biomass for each organ; (ii) we conducted the curve fitting of the calculated ratios in (i). Figure 3 shows the calculated ratios of glucose partitioned to each organ and the fitting curves for the ratios.

To determine the ratio of dead leaf at harvest ($r_{d1,lef}$), we first calculated the observational ratios of dead leaf during growing period by dividing the decrease in leaf biomass between observational dates by the duration among the observational dates. Then by graphically fitting a curve to the calculated ratios of dead leaf, we determined $r_{d1,lef}$. Figure 4 shows the calculated ratios of dead leaf and the fitted curve.

The fraction of glucose allocated to starch reserve (f_{stc}) is determined as follows: (i) we first calculated the ratios of stem biomass at harvest to maximum stem biomass for each year from 2003 to 2006 (Bouman et al. (2001)); (ii) then, a 4-year average was calculated for f_{stc}.

3.4 LAI, height, and specific leaf weight

To obtain the parameters for the relationship between LAI and crop height ($h_{gt,aa}, h_{gt,ab}, h_{gt,ba}$, and $h_{gt,bb}$), we conducted linear regressions of the data before and after heading using observations for LAI and crop height from 2003 to 2006. Thus, $h_{gt,aa} = 0.439, h_{gt,ab} = 0.675, h_{gt,ba} = 0.366$, and $h_{gt,bb} = 0.318$. Figure 5 compares the LAI–height relation between observations and simulations.

To obtain parameters for specific leaf weight (k_{SLW}, SLW_{mn}, and SLW_{mx}), we plotted observations for specific leaf weights during growing periods from 2003 to 2006 and conducted the curve fitting of the plotted data. Thus, $k_{SLW} = 3.5, SLW_{mn} = 350$, and $SLW_{mx} = 600$. Figure 6 shows the specific leaf weights and the fitted curve.

3.5 Crop yield

To determine the ratio of crop yield to dry weight of panicle at harvest (k_{yld}), we calculated the dry weight of panicle at harvest, because the weight was not observed. By assuming linear increase of dry weight from the last date in which dry weight of the panicle was measured, we calculated the dry weight of the panicle at harvest from 2003 to 2006. The median value among the ratios of observed yields to the calculated dry weight of panicle produced k_{yld}.

Geosci. Model Dev. Discuss., doi:10.5194/gmd-2016-29, 2016
Manuscript under review for journal Geosci. Model Dev.
Published: 19 February 2016

Geoscientific Model Development Discussions

4 Validation

4.1 LHF and SHF

Figures 7 and 8 show the comparison of the daily LHF and SHF, respectively, during growing periods between observations and simulations from 2003 to 2006. We can observe that MATCRO can replicate daily variations in LHF and SHF accurately. Quantitatively, the RMSEs of LHF between simulations and observations for each year were 16.25, 21.56, 19.38, and 17.38 W m^{-2}, with the 4-year average of 18.57 W m^{-2}. The RMSEs of SHF were 12.29, 18.94, 10.90, and 8.97 W m^{-2}, with the 4-year average of 12.66 W m^{-2}. These RMSE values are comparable to those reported in earlier studies (Kimura and Kondo,1998; Maruyama and Kuwagata,2010).

One of the major reasons for the errors of LHF and SHF between simulations and observations is thought to be a problem in flux observations. Aubinet et al. (2000) reported that the energy balance in observations is not closed. In contrast, the energy balance simulated by MATCRO is completely closed. Therefore, the energy imbalance in flux observations can cause errors between simulations and observations. El Maayar et al. (2008) suggested to test the degree of energy imbalance in observations before comparing the observations with simulations. This degree is generally evaluated by

$$I_m = \left(\sum_d \frac{(\overline{H}(d) + \lambda\overline{E}(d))}{(\overline{R}_n(d) - \overline{G}(d))} \right) / N, \quad (1)$$

where $\overline{H}$, $\lambda\overline{E}$, $\overline{R}_n$, and $\overline{G}$ are the daily averages for SHF, LHF, net radiation, and heat flux into ground, respectively, d indicates a day, and N is the number of days. The observation values for R_n and G in this equation are expected to be sufficiently accurate (Twine et al., 2000; Wilson et al., 2002). The values of I_m in the observations from 2003 to 2006 were 0.78, 0.78, 0.78, and 0.74, with the average of 0.77. In other words, these results imply that the total flux of observed LHF and SHF can be smaller than a true value. Therefore, it is desirable that the total flux of simulated SHF and LHF is approximately 1.3-fold (= 1/0.77) larger than the observation values. The total values of the simulated SHF and LHF from 2003 to 2006 were on average 1.16-fold larger than the observations. This suggests that the errors of LHF and SHF between observations and simulations can be largely attributed to the energy imbalance in observations.

4.2 Net carbon flux

In this section, we tested the accuracy of MATCRO for simulating net carbon flux during growing periods by comparing the changes in total biomass between simulations and observations. Figure 9 compares the growth of the total biomass between simulations and observations from 2003 to 2006. As indicated by the figure, the simulated total biomass was in good agreement with the observations. Hence, we conclude that the model has high accuracy for simulating net carbon flux during growing period. However, the model overestimated the total biomass in the middle of the growth stage in 2005 and underestimated the total biomass in the late growth stage in 2004. Hence, several model improvements are needed.

Geosci. Model Dev. Discuss., doi:10.5194/gmd-2016-29, 2016
Manuscript under review for journal Geosci. Model Dev.
Published: 19 February 2016

4.3 Yield

Figure 10 shows the comparison of the observed and simulated yields from 2003 to 2006. As indicated by the figure, MATCRO can reproduce well the absolute values of crop yields. The mean RMSE from 2003 to 2006 was 402.4 kg ha^{-1}, which was 7.9% of the mean observed yields. However, the model overestimated the crop yields in 2003. The primary cause of the large overestimation in 2003 can be attributed to the late harvest in the simulation for 2003; the model delayed the harvest by 11 days in 2003 (see Section 3.2). To confirm this, we recalculated the yield in 2003 by using the observed harvest date. The revised yield is shown in the figure as a red circle. The revised yield was in good agreement with the observations in 2003. These results suggest that the phenological model in MATCRO should be further improved for a more accurate estimation of crop yield. The current version of the phenological model in MATCRO implements only the temperature. The consideration of the photoperiod may further improve the accuracy of the phenological model in the simulation of harvest date as well as heading date (e.g., Penning de Vries et al., 1989; Connor et al. ,2011).

5 Concluding remarks

In this paper, we presented the results of the validation of MATCRO-Rice as well as of the numeric and parameterisation methods. First, the comparison of the LHF and SHF between simulations and observations confirmed that the model can reproduce the observed LHF and SHF data well. The accuracy of the simulations for LHF and SHF was comparable to those obtained in earlier studies. Second, we showed that the simulated growth of the total biomass was in good agreement with the observations. This indicates that the model can simulate the net carbon flux during a growing period at paddy rice fields. Last, we demonstrated that the model has high ability to simulate crop yield by comparing the simulated and observed yields. In addition, it was found that improvement of the phenological model is necessary for more accurate simulation of the yield.

The validation results suggest that MATCRO-Rice has high ability to accurately and consistently simulate LHF, SHF, net carbon flux, and yield. There have been many models that simulate some of the four variables with high accuracy, but a few models can accurately and consistently simulate all four of them. This point is the most important feature of MATCRO-Rice. The model can be applied to a wide range of issues, including climate change impact (e.g., Masutomi et al.,2009), and it will facilitate the scientific research especially on the climate–crop interactions (Osborne et al.,2009).

We validated this model with observations from only one site. The model should be further validated at multiple sites in order to enforce the reliability and applicability of the model. However, since there are a few flux sites on agriculture land worldwide, it will be necessary to increase their number on agricultural land to promote climate–crop modelling studies.

6 Code availability

The source code of MATCRO will be distributed at request to the corresponding author (Yuji Masutomi: yuji.masutomi@gmail.com). The website for MATCRO-Rice will be developed in the near future.

Geosci. Model Dev. Discuss., doi:10.5194/gmd-2016-29, 2016
Manuscript under review for journal Geosci. Model Dev.
Published: 19 February 2016

Acknowledgements. We are grateful to Mrs Hatanaka for her help in extensive literature survey. This research was supported by the Environment Research and Technology Development Fund (S-12) and the Program on Development of Regional Climate Change Adaptation Plans in Indonesia (PDRCAPI) of the Ministry of the Environment.

Geosci. Model Dev. Discuss., doi:10.5194/gmd-2016-29, 2016
Manuscript under review for journal Geosci. Model Dev.
Published: 19 February 2016

References

AsiaFlux: MSE: Mase paddy flux site, http://asiaflux.net/index.php?page_id=83, Accessed on Feb. 5, 2016.

Aubinet, M., Grelle, A., Ibrom, A., Rannik, Ü., Moncrieff, J., Foken, T., Kowalski, A. S., Martin, P. H., Berbigier, P., Bernhoffer, Ch., Clement, R., Elbers, J., Granier, A., Grünwald, T., Morgenstern, K., Pilegaard, K., Rebmann, C., Snijders, W., Valentini, R., and Vesala, T.: Estimates of the annual net carbon and water exchange of forests: the EUROFLUX methodology. Adv. Ecol. Res., 30, 113-175, 1999.

Betts, R. A.: Integrated approaches to climate-crop modelling: needs and challenges, Phil. Trans. R. Soc. B, 360, 2049-2065, 2005.

Bondeau, A., Smith, P. C., Zaehle, S., Schaphoff, S., Lucht, W., Cramer, W., Gerten, D., Lotze-Campen, H., Müller, C., Reichstein, M., and Smith, B.: Modelling the role of agriculture for the 20th century global terrestrial carbon balance, Glob. Change Biol., 13, 679-706, 2007.

Borjigidai, A., Hikosaka, K., Hirose, T., Hasegawa, T., Okada, M., and Kobayashi, K.: Seasonal changes in temperature dependence of photosynthetic rate in rice under a free-air CO_2 enrichment, Ann. Bot., 97, 549-557, 2006.

Bouman, B. A. M., Kropff, M. J., Tuong, T. P., Wopereis, M. C. S., ten Berge, H. F. M., and van Laar, H. H.: ORYZA2000: modeling lowland rice, International Rice Research Institute and Wageningen University and Research Centre, Phillippines and Wageningen, 2001.

Campbell, G. S., and Norman, J. M.: An introduction to environmental biophysics, Springer-Verlag, New York, 1998.

Connor D. J., Loomis, R. S., and Cassman, K. G.: Crop ecology: productivity and management in agricultural systems, Cambridge University Press, Cambridge, 2011.

Gervois, S., de Noblet-Ducoudré, N., Viovy, N., Ciais, P., Brisson, N., Seguin, B., and Perrier, A.: Including croplands in a global biosphere model: methodology and evaluation at specific sites, Earth Interact., 8, 1-25, 2004.

El Maayar, M., Chen, J. M., and Price, D. T.: On the use of field measurements of energy fluxes to evaluate land surface models, Ecol. Model., 214, 293-304, 2008.

Kimura, R., and Kondo, J.: Heat balance model over a vegetated area and its application to a paddy filed. J. Meteorol. Soc. Jpn., 76, 937-953, 1998.

Kucharik, C. J.: Evaluation of a process-based agro-ecosystem model (Agro-IBIS) across the U.S. corn belt: simulations of the interannual variability in maize yield, Earth Interact., 7, 1-33, 2003.

Lei, H., Yang, D., Lokupitiya, E., and Shen, Y.: Coupling land surface and crop growth models for predicting evapotranspiration and carbon exchange in wheat-maize rotation croplands, Biogeosciences, 7, 3363-3375, 2010.

Levis, S, Bonan, G. B., Kluzek, E., Thornton, P. E., Jones, A., Sacks, W. J., and Kucharik, C. J.: Interactive crop management in the Community Earth System Model (CESM1): Seasonal influences on land-atmosphere fluxes, J. Climate, 25, 4839-4859, 2012.

Lokupitiya, E., Denning, S., Paustian, K., Baker, I., Schaefer, K., Verma, S., Meyers, T., Bernacchi, C. J., Suyker, A., and Fischer, M.: Incorporation of crop phenology in Simple Biosphere Model (SiBcrop) to improve land-atmosphere carbon exchanges from croplands, Biogeosciences, 6, 969-986, 2009.

Maruyama, A., and Kuwagata, T.: Coupling land surface and crop growth models to estimate the effects of changes in the growing season on energy balance and water use of rice paddies, Agr. Forest Meteorol., 150, 919-930, 2010.

Masutomi, Y., Takahashi, K., Harasawa, H., and Matsuoka, Y.: Impact assessment of climate change on rice production in Asia in comprehensive consideration of process/parameter uncertainty in general circulation models, Agric. Ecosys. Environ., 131, 281-291, 2009

Masutomi, Y., Ono, Mano, M., Maruyama, A., and Miyata, A.: A land surface model combined with a crop growth model for paddy rice (MATCRO-Rice Ver. 1) – Part I: Model description, 2016 (submitted to Geosci. Model Dev. Discuss.)

Nelder, J. A., and Mead, R.: A simplex method for function minimization, Comput. J., 7, 308-313, 1965.

Geosci. Model Dev. Discuss., doi:10.5194/gmd-2016-29, 2016
Manuscript under review for journal Geosci. Model Dev.
Published: 19 February 2016

Oki, T., and Kanae, S.: Global hydrological cycles and world water resources, Science, 313, 1068-1072, 2006.

Osborne, T. M., Lawrence, D. M., Challinor, A. J., Slingo, J. M., and Wheeler, T. R.: Development and assessment of a coupled crop-climate model, Glob. Change Biol., 13, 169-183, 2007.

Osborne, T. M., Slingo, J., Lawrence, D., Wheeler, T.: Examining the interaction of growing crops with local climate using a coupled crop-climate model, J. Climate, 22, 1393-1411, 2009.

Osborne, T., Gornall, J., Hooker, J., Williams, K., Wiltshire, A., Betts, R., and Wheeler, T.: JULES-crop: a parametrisation of crops in the Joint UK Land Environment Simulator, Geosci. Model Dev., 8, 1139-1155, 2015.

Penning de Vries, F. W. T., Jansen, D. M., ten Berge, H. F. M., and Bakema, A.: Simulation of ecophysiological processes of growth in several annual crops, Centre for Agricultural Publishing and Documentation (Poduc), Wageningen, 1989.

Saxton, K. E., and Rawls, W. J.: Soil water characteristic estimates by texture and organic matter for hydrologic solutions. Soil Sci. Soc. Am. J. 70, 1569-1578, 2006.

Takata, K., Emori, S., and Watanabe, T.: Development of the minimal advanced treatments of surface interaction and runoff. Global Planet. Change, 38, 209-222, 2003.

Tsvetsinskaya, E. A., Mearns, L. O., and Easterling, W. E.: Investigating the effects of seasonal plant growth and development in three-dimensional atmospheric simulations. Part II: Atmospheric response to crop growth and development, J. Climate, 14, 711-729, 2001.

Twine, T. E., Kustas, W. P., Norman, J. M., Cook, D. R., Houser, P. R., Meyers, T. P., Prueger, J. H., Starks, P. J., and Wesely, M. L.: Correcting eddy-covariance flux underestimates over a grassland, Agr. Forest Meteorol., 103, 279-300, 2000.

Wilson, K. B., Baldocchi, D. D., Aubinet, M., Berbigier, P., Bernhofer, Ch., Dolman, H., Falge, E., Field, C., Goldstein, H., Granier, A., Grelle, A., Halldor, T., Hollinger, D., Katul, G., Law, B. E., Lindroth, A., Meyers, T., Moncrieff, J., Monson, R., Oechel, W., Tenhunen, J., Valentini, R., Verma, S., Vesala, T., and Wofsy, S.: Surface energy partitioning between latent and sensible heat flux at FLUXNET sites, Water Resour. Res., 38, 1294, 2002.

Geosci. Model Dev. Discuss., doi:10.5194/gmd-2016-29, 2016
Manuscript under review for journal Geosci. Model Dev.
Published: 19 February 2016

Geoscientific Model Development Discussions
Open Access
EGU

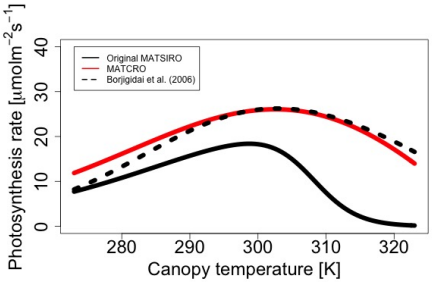

Figure 1. Rubisco-limited photosynthesis rate

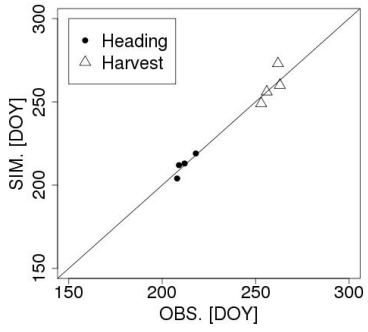

Figure 2. Comparison of heading and harvest dates. SIM: simulations; OBS: observations; DOY: The number of days from Jan. 1.

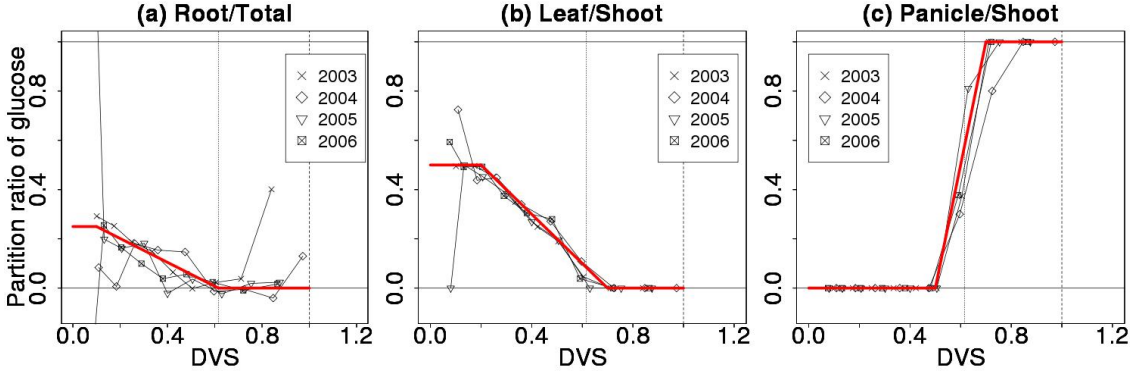

Figure 3. Partitioning ratio of glucose. Red lines are fitted. DVS: dynamics vegetation model

Geosci. Model Dev. Discuss., doi:10.5194/gmd-2016-29, 2016
Manuscript under review for journal Geosci. Model Dev.
Published: 19 February 2016

Geoscientific Model Development Discussions
Open Access
EGU

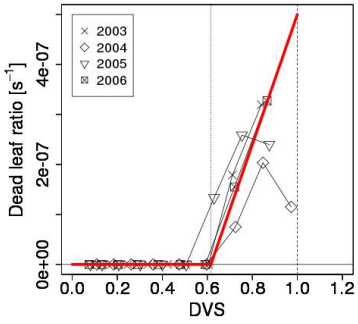

Figure 4. Ratio of dead leaf. DVS: dynamics vegetation model

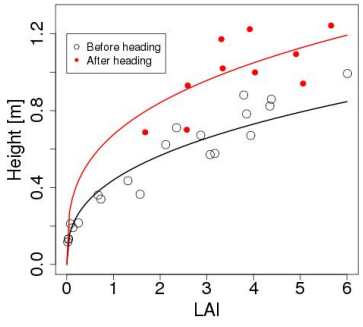

Figure 5. Relationship between the leaf area index (LAI) and crop height (black curve: $h = h_{gt,aa} L^{h_{gt,ab}}$; red curve: $h = h_{gt,ba} L^{h_{gt,bb}}$)

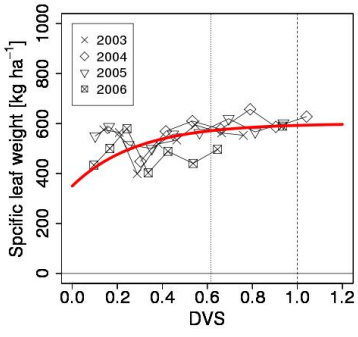

Figure 6. Relationship between specific leaf weight and dynamics vegetation model (DVS)

Geosci. Model Dev. Discuss., doi:10.5194/gmd-2016-29, 2016
Manuscript under review for journal Geosci. Model Dev.
Published: 19 February 2016

Geoscientific Model Development Discussions
Open Access
EGU

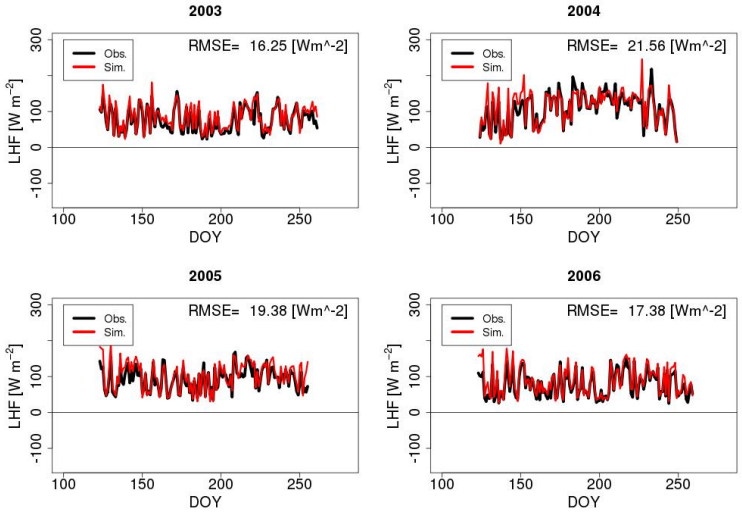

Figure 7. Comparison of latent heat flux (LHF) between simulations and observations. DOY:

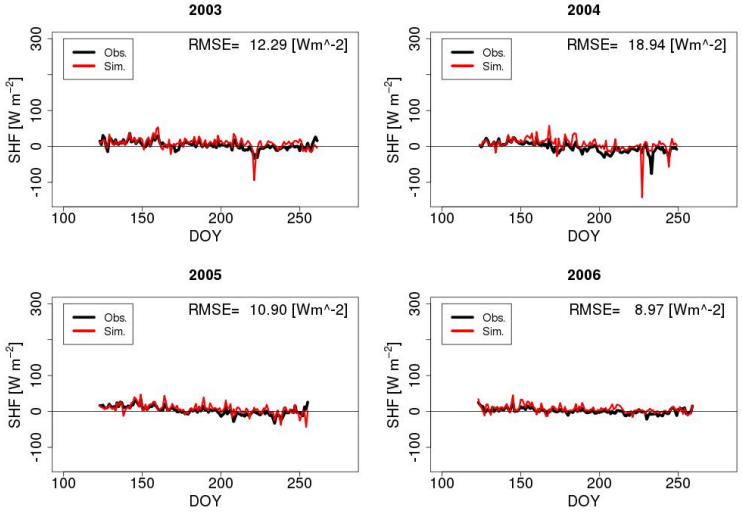

Figure 8. Comparison of sensible heat flux (SHF) between simulations and observations

Geosci. Model Dev. Discuss., doi:10.5194/gmd-2016-29, 2016
Manuscript under review for journal Geosci. Model Dev.
Published: 19 February 2016

Geoscientific Model Development Discussions

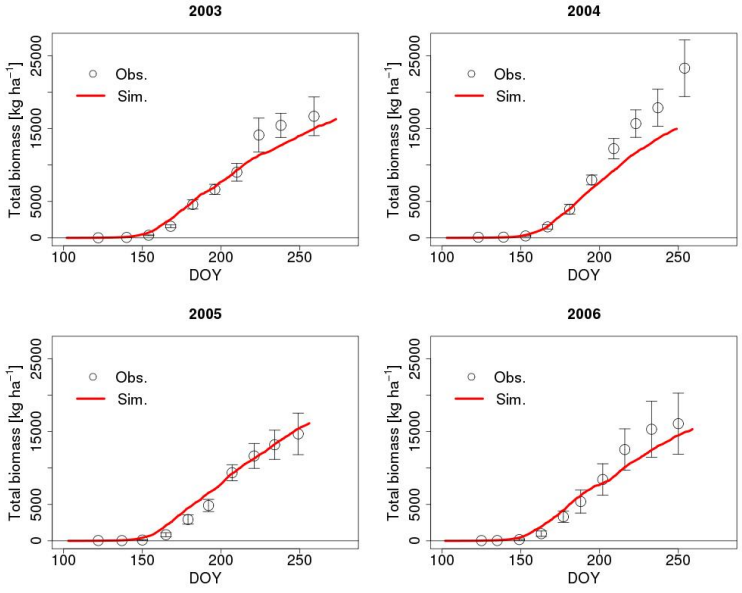

Figure 9. Comparison of total biomass between simulations and observations during growing periods from 2003 to 2006. Circles indicate mean values of observations and the ranges indicate standard deviation of observations. Red lines denotes simulations. DOY:

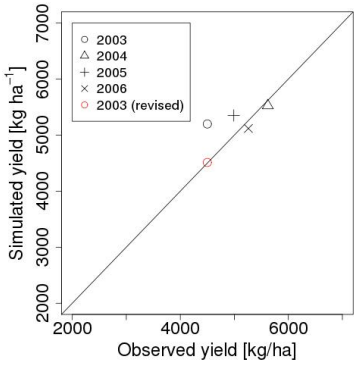

Figure 10. Comparison of yields between simulations and observations

Table 1. Soil-type specific parameters

Variable	Value	Unit	Description	Source
B	5.2	-	factor for hydraulic conductivity and water potential	Campbell and Norman (1998)
K_s	0.000064	kg s m^{-3}	hydraulic conductivity at saturation	Campbell and Norman (1998)
w_{sat}	0.48	m^3 m^{-3}	volumetric concentration of soil water at saturation	Saxton and Rawls (2006)
ψ_s	-2.6	J kg^{-1}	water potential at saturation	Campbell and Norman (1998)
ρ_s	1390	kg m^{-3}	bulk density of soil	Saxton and Rawls (2006)

Geosci. Model Dev. Discuss., doi:10.5194/gmd-2016-29, 2016
Manuscript under review for journal Geosci. Model Dev.
Published: 19 February 2016

Geoscientific Model Development Discussions
Open Access
EGU

Table 2. Observational data

Variable	Unit	Description
Meteorological inputs		
P_a	Pa	Air pressure
P_r	kg m^{-2} s^{-1}	Precipitation
Q	kg kg^{-1}	Specific humidity
$R_s^d(0)$	W m^{-2}	Downward shortwave radiant flux density at the canopy top
$R_l^d(0)$	W m^{-2}	Downward longwave radiant flux density at the canopy top
T_a	K	Air temperature
U	m s^{-1}	Wind speed
$D_1^d(0) + S_1^d(0)$	W m^{-2}	Downward radiant flux density for photosynthesis active radiation at the canopy top
Outputs		
λE	W m^{-2}	Latent heat flux
H	W m^{-2}	Sensible heat flux
$W_{sh} + W_{rot}$	kg ha^{-1}	Total biomass
Yld	kg ha^{-1}	Yield
Parameterisation		
L	m$^2(l)$ m^{-2}	Leaf area index
Tr_{DOY}	day	the number of days of transplanting from Jan. 1
Hd_{DOY}	day	the number of days of heading from Jan. 1
Hv_{DOY}	day	the number of days of harvest from Jan. 1
h	m	Crop height
W_{lef}	kg ha^{-1}	dry matter weight of leaf
W_{stm}	kg ha^{-1}	dry matter weight of stem
W_{rot}	kg ha^{-1}	dry matter weight of root
W_{pnc}	kg ha^{-1}	dry matter weight of panicle

Geosci. Model Dev. Discuss., doi:10.5194/gmd-2016-29, 2016
Manuscript under review for journal Geosci. Model Dev.
Published: 19 February 2016

Geoscientific Model Development Discussions
Open Access
EGU

Table 3. Simulation setting parameters

Variable	Value	Unit	Description
C_a	390	ppm	atmospheric CO_2 concentration
d_w	0.025	m	depth of surface water
L_{at}	36.05	degree	latitude at simulation site
Sw_{DOY}	$Tr_{DOY} - 20$	day	the number of days of sowing from Jan. 1
$W_{glu,0}$	0.5	kg ha^{-1}	dry weight of glucose reserve at emergence
$W_{lef,0}$	1.0	kg ha^{-1}	dry weight of leaf at emergence
$W_{rot,0}$	1.0	kg ha^{-1}	dry weight of root at emergence
$W_{stm,0}$	1.0	kg ha^{-1}	dry weight of stem at emergence
z_a	3	m	reference height at which wind speed is observed
z_{max}	4	m	depth of soil layer
z_{sat}	0.05	m	depth to which soil is saturated
z_b	2	m	depth from the soil surface to the upper bound of the bottommost layer of soil
δt	1800	s	time resolution

Geosci. Model Dev. Discuss., doi:10.5194/gmd-2016-29, 2016
Manuscript under review for journal Geosci. Model Dev.
Published: 19 February 2016

Geoscientific Model Development Discussions
Open Access
EGU

Table 4. Parameters parameterised

Variable	Value	Unit	Description
DVS_{rot1}	0.1	-	1st point of DVS at which the partition pattern to root changes
DVS_{rot2}	$hDVS$	-	2nd point of DVS at which the partition pattern to root changes
DVS_{lef1}	0.2	-	1st point of DVS at which the partition pattern to leaf changes
DVS_{lef2}	0.7	-	2nd point of DVS at which the partition pattern to leaf changes
DVS_{pnc1}	0.5	-	1st point of DVS at which the partition pattern to panicle changes
DVS_{pnc2}	0.7	-	2nd point of DVS at which the partition pattern to panicle changes
$eDVS$	0.012	-	DVS at emergence
f_{stc}	0.288	-	fraction of glucose allocated to starch reserves
h_{aa}	0.439	-	parameter for relationship between LAI and height before heading
h_{ab}	0.675	-	parameter for relationship between LAI and height before heading
h_{ba}	0.366	-	parameter for relationship between LAI and height after heading
h_{bb}	0.318	-	parameter for relationship between LAI and height after heading
$hDVS$	0.616	-	DVS at heading
k_{yld}	0.675	-	ratio of crop yield to dry weight of panicle at maturity
k_{SLW}	3.5	-	parameter that represent the relationship between SLW and DVS
$mGDS$	167759940	K· s	growing degree second at maturity
P_{rot}	0.25	-	partition ratio of glucose to root
P_{lef}	0.5	-	partition ratio of glucose to leaf from glucose partitioned to shoot
$r_{d1,lef}$	5.0 * 10^{-7}	s^{-1}	ratio of leaf death at harvest
SLW_{mx}	600	kg m^{-2}	maximum specific leaf area
SLW_{mn}	350	kg m^{-2}	minimum specific leaf area
s_1	0.045	K^{-1}	temperature dependence of $\overline{V}_{max,x}$on $\overline{V}_{m,x}$
s_2	328	K	temperature dependence of $\overline{V}_{max,x}$ on $\overline{V}_{m,x}$
$V_{max}(0)$	0.001	mol $m^{-2}(l)$ s^{-1}	reference value for maximum Rubisco capacity at the canopy top
$trDVS$	0.06	-	DVS at transplanting and at which transplanting shock starts
$teDVS$	0.08	-	DVS at which transplanting shock ends